PHY 4210-01 Senior Lab
Lab N4: Rutherford Scattering

Sarah Arends
Jacquelyne Miksanek
Ryan Wojtyla

Instructor: Dr. Marcus Hohlmann

March 14, 2019

Abstract

A Rutherford scattering process is studied by placing an Americium 241 source in a vacuum chamber and sending a collimated beam towards a Gold or Aluminum foil. The counting rate is measured at various scattering angles, and the corrected counting rate with respect to the scattering distribution is calculated and compared to the Rutherford scattering rate. The differential cross section is also calculated and compared to a theoretical value.

Contents

1 Objective of the Experiment

During this experiment, the differential cross-section for a scattering process will be determined. Researchers will measure the counting rate for alpha particles scattered by a Gold or Aluminum foil as a function of the angle at which it is scattered. Using this information, one can calculate a counting rate corrected with respect to the scattering distribution. The following Rutherford scattering formula can then be validated:

$$N(\theta) = N_0 \times c_F \times d_f \times \frac{Z^2 \times e^4}{\left(8\pi \times \epsilon_0 \times E_\alpha\right)^2 \times sin^4\left(\frac{\theta}{2}\right)} \tag{1}$$

2 Theory of the Experiment

Rutherford scattering describes the process in which charged particles undergo elastic scattering due to a Coulomb force interaction. When the positively charged alpha particles approach the positively charged gold nuclei, the like charges cause a repulsive force that deflects the alpha particles at varying angles. This deflection/scattering angle depends on the distance of closest approach between the alpha particles and nuclei, since the Coulomb force is a function of distance. Because the gold atoms consist of mostly empty space, the majority of alpha particles are sufficiently far away from the gold nuclei that they experience minimal Coulomb repulsion and are only scattered at angles of less than one degree. However, there are still some alpha particles that approach the gold nuclei close enough to experience stronger Coulomb repulsion and scattering at greater angles. If one were to observe the number of scattered alpha particles as a function of the angle at which they are scattered, the resultant distribution would show a large rate at small angles, but the distribution would quickly drop off as the angle increases. Note, however, that this distribution does not account for particles that are back-scattered, meaning that they are close enough to the gold nuclei to be deflected backwards towards the alpha source. Accounting for these measurements would show a spike in the rate curve at an angle of 180 degrees, in what is otherwise a monotonically decreasing distribution.

When an alpha particle with impact parameter b approaches a nucleus, it is scattered at an angle θ. If the impact parameter is given an infinitesimal range of [b, $b + db$], the resulting scattering angle then has a range of [$\theta - d\theta$, θ]; the impact parameter and scattering angle are inversely proportional.

Because the alpha particle can be incident within a defined range at any angle relative to the nucleus, a ring of possible incident locations is created in front of the nucleus. This ring is illustrated in Figure 1.

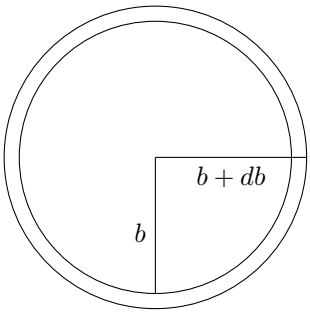

Figure 1: The ring whose area represents the possible region in which alpha particles may be incident on a target nucleus.

The area of this ring is found as the area of any ring is found:

$$\begin{aligned} A &= \pi(b+db)^2 - \pi b^2 \\ &= \pi(b^2 + 2bdb + db^2) - \pi b^2 \\ &= \pi b^2 + 2\pi bdb + \pi db^2 - \pi b^2 \\ &= 2\pi bdb + \pi db^2 \end{aligned}$$

Since db is infinitesimally small, it can be approximated to be zero. Therefore, the area of the incident ring, $\Delta\sigma$, is

$$\Delta\sigma = 2\pi bdb \tag{2}$$

Since the impact parameter b is directly proportional to the size of the cross section and the scattering angle θ is inversely proportional to the impact parameter, the size of the cross section decreases as the scattering angle increases. Therefore, the cross section experiences a negative rate of change as θ increases. Hence,

$$\Delta\sigma(\theta) = -d\sigma(\theta) \tag{3}$$

The circumference of a circle is equal to $2\pi r$, where r is the radius of the circle. In the experiment, the radius of the ring onto which the alpha particle is projected after it is scattered is $R\sin(\theta)$, where θ is the scattering angle and R, described in Figure 2, is the distance between the point at which the alpha particle was scattered and the edge of the ring.

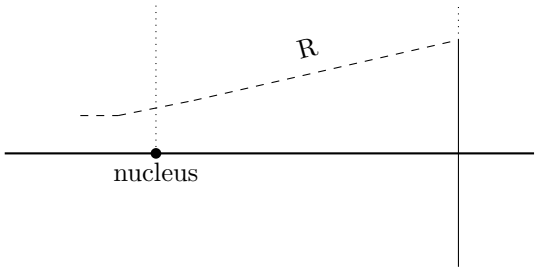

Figure 2: The path of the alpha particle as it is scattered by a nucleus. R is the path length between the nucleus and the ring of the solid angle.

The outer circumference of this ring is $2\pi R\sin(\theta)$. Since the alpha particle is incident within a range whose minimum is $\theta - d\theta$, however, the ring has a thickness of $Rd\theta$. Since the thickness of the ring is infinitesimal, the ring's area can be approximated to be that of a rectangle. Therefore, the area of the ring is $A = 2\pi R\sin(\theta)Rd\theta$.

The solid angle of the scattered alpha particles at an angle θ is:

$$\begin{aligned}\Delta\Omega &= \frac{A}{R^2} \\ &= \frac{(2\pi R\sin(\theta)Rd\theta)}{R^2}\end{aligned}$$

$$d\Omega = 2\pi\sin(\theta) \tag{4}$$

An expression for the differential cross section $\frac{d\sigma}{d\Omega}(\theta)$ can be found by multiplying Equation 2 by Equation 2 divided by itself.

$$\begin{aligned}\Delta\sigma &= -\frac{d\sigma}{d\Omega}(\theta)d\Omega \\ &= -\frac{d\sigma}{d\Omega}(\theta)2\pi\sin(\theta)d\theta\end{aligned}$$

From Equation 2:

$$-\frac{d\sigma}{d\Omega}(\theta)2\pi\sin(\theta)d\theta = 2\pi bdb$$

$$\frac{d\sigma}{d\Omega}(\theta) = -\frac{b}{\sin(\theta)}\frac{db}{d\theta} \tag{5}$$

Since it is known that $b = \frac{ZZ'e^2}{2E}\cot\left(\frac{\theta}{2}\right)$, it can be inserted into Equation 2. Furthermore, since b is a function of θ, $\frac{db}{d\theta}$ can also be found:

$$\begin{aligned} b &= \frac{ZZ'e^2}{2E}\cot\left(\frac{\theta}{2}\right) \\ \frac{db}{d\theta} &= \frac{ZZ'e^2}{2E}\left(-\frac{1}{2}\csc^2\left(\frac{\theta}{2}\right)\right) \\ \frac{db}{d\theta} &= -\frac{ZZ'e^2}{4E}\csc^2\left(\frac{\theta}{2}\right) \end{aligned}$$

Now that b and db have been found, the full expression for the differential cross section $\frac{d\sigma}{d\Omega}$ can be determined:

$$\begin{aligned} \frac{d\sigma}{d\Omega}(\theta) &= -\frac{b}{\sin(\theta)}\frac{db}{d\theta} \\ &= -\left(\frac{ZZ'e^2}{2E}\cot\left(\frac{\theta}{2}\right)\right)\frac{1}{\sin(\theta)}\left(-\frac{ZZ'e^2}{4E}\csc^2\left(\frac{\theta}{2}\right)\right) \\ &= 2\left(\frac{ZZ'e^2}{4E}\right)^2\frac{\cos\left(\frac{\theta}{2}\right)}{\sin\left(\frac{\theta}{2}\right)}\frac{1}{\sin(\theta)}\frac{1}{\sin^2\left(\frac{\theta}{2}\right)} \\ &= 2\left(\frac{ZZ'e^2}{4E}\right)^2\cos\left(\frac{\theta}{2}\right)\frac{1}{\left(2\sin\left(\frac{\theta}{2}\right)\cos\left(\frac{\theta}{2}\right)\right)}\frac{1}{\sin^3\left(\frac{\theta}{2}\right)} \end{aligned}$$

$$\frac{d\sigma}{d\Omega}(\theta) = \left(\frac{ZZ'e^2}{4E}\right)^2\frac{1}{\sin^4\left(\frac{\theta}{2}\right)} \tag{6}$$

Equation 2 is the equation for calculating the theoretical differential cross-section.

The differential cross-section can also be found experimentally using a measured alpha particle scattering rate at a particular angle θ. First, this relation must be constructed. The collimated beam of alpha particles begins its journey with an incident rate of $\frac{dN_0}{dt}$. This beam is then incident on a thin foil with an atomic density of $n = \frac{\rho N_A d}{A}$, where ρ is the density of the foil material, d is the thickness of the foil, and A is the atomic number of the foil material. Being incident on the foil, the alpha particles are exposed to a differential cross-section at the particular angle of $\frac{d\sigma}{d\Omega}(\theta)$. The alpha particles are scattered by the nuclei across a solid angle $\Delta\Omega = A_{\text{detector}}r^2$, where A_{detector} is the area of the detector and r is the distance between the foil and detector. Multiplying these factors together results in the scattering rate of the alpha particles incident on a particular foil at a particular angle: $\frac{dN}{dt}(\theta) = \frac{dN_0}{dt}n\frac{d\sigma}{d\Omega}(\theta)\Delta\Omega$. Since the scattering rate is determined experimentally, the equation can be rearranged for the differential cross-section:

$$\frac{d\sigma}{d\Omega}(\theta) = \frac{\frac{dN}{dt}(\theta)}{\frac{dN_0}{dt}n\Delta\Omega} \tag{7}$$

As you can see from equation 2, the angluar dependence of the function is $\frac{1}{\sin^4\left(\frac{\theta}{2}\right)}$. This implies that the curve of the function drops off rather quickly at larger angles due to this term, therefore, the rate drops off quickly as well.

3 Equipment Utilized

A series of readout electronics are used to process the signal from a photodiode detector, including: a pre-amplifier, an amplifier, a discriminator, and a counter. An oscilloscope was used to verify the signal behavior at various points in the circuit. The scattering chamber, where the Rutherford scattering process was performed, required evacuation with a vacuum pump. A rotating arm inside the chamber contains an Americium 241 source, a collimating slit, a Gold or Aluminum foil, and the photodiode. A photodiode detects the energy of the alpha particle and returns an electrical signal, which is then transmitted through the aforementioned readout electronics. A more detailed description of the experimental process and implementation of this equipment can be found in the Procedure section of this report. The following list summarizes the pieces of equipment used and some relevant specifications:

- Rutherford scattering chamber
- Aluminum foil in frame:
  Molar mass 27 g/mol
  Thickness 1.50×10^{-7} m
  Density 2.70×10^{6} g/m^3
- Gold foil in frame:
  Molar mass 197 g/mol
  Thickness 2.00×10^{-8} m
  Density 1.93×10^{7} g/m^3
- Vacuum pump, for evacuating scattering chamber
- Readout modules:
  Discriminator, Amplifier, Preamplifier, Counter
- ^{241}Americium (alpha source)
- Oscilloscope, for monitoring signals on readout modules
- Photodiode detector
  Width 2.22×10^{-3} m
  Height 4.12×10^{-3} m
- Collimating slit
  Width 0.005 m

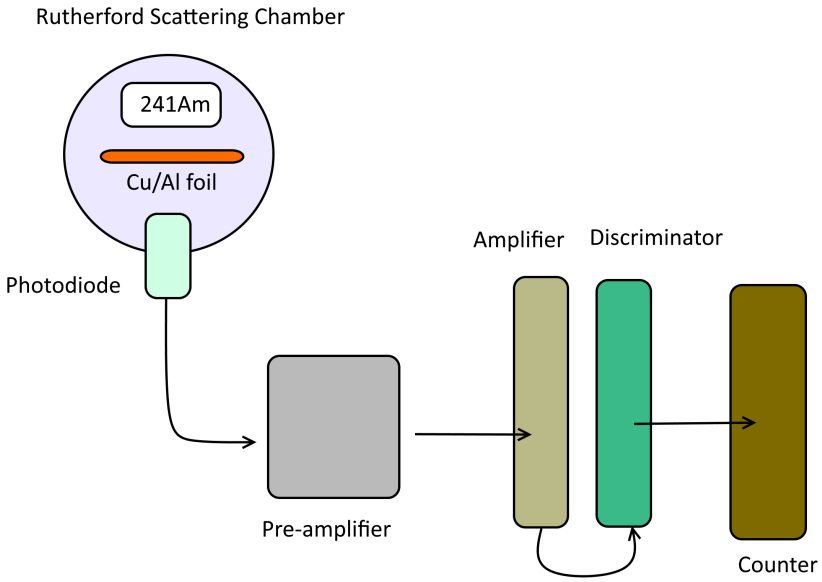

Figure 3: Schematic for circuit diagram

4 Procedure

Alpha particles are produced from an ^{241}Am source mounted inside the vacuum chamber on a rotating arm. Also mounted on this arm, directly in front of the source, is a collimating slit followed by a thin gold foil. With this configuration, one is able to strike the gold foil with a uniform, collimated beam of alpha particles. The chamber must be evacuated using an external vacuum pump, since alpha particles have a very short lifetime in air.

Alpha particles are scattered by Gold nuclei at varying angles, and the scattered particles are detected using a photodiode. In order to determine the dependence of the scattering rate on the incident angle, the rotating arm was moved through a range of -30 degrees to 30 degrees using a knob on top of the vacuum chamber. Here, an angle of 0 degrees represents the arm oriented along the same line as the photodiode. Because the Gold foil is incredibly thin, any air movement resulting from the utilization of the vacuum pump can potentially damage the foil. To mitigate this risk, the pump must be opened and closed slowly. The plane of the Gold foil is also oriented parallel to the valve's tube during this process so that the foil does not impede air flow and result in a tear of the foil.

The photodiode is connected via an external BNC port to a pre-amplifier that shapes the measurement signal. This is then connected to an amplifier, which amplifies the signal in accordance with a prescribed gain. This amplified signal is fed to a discriminator, which sets a minimum/threshold voltage in order to differentiate meaningful signals from electronic noise. Signals that meet this

threshold are output in the form of a digital pulse. These pulses are fed to a counter module, which reads out the number of pulses over a given time interval. The count rate decreases dramatically as the scattering angle increases. For this reason, the acquisition time was increased for larger angles in order to obtain sufficient statistics. The experimental scattering rate can be used to calculate the differential cross-section.

4.1 Procedural Modifications

The manual dictates that the chamber be evacuated using the vacuum pump before conducting trials. However, it was determined that the seal of the vacuum chamber was not sufficient, and the detected rate of alpha particles would dramatically decrease after a few minutes. Therefore, in order to maintain a true vacuum throughout the course of data taking, the pump was continually operated throughout the experiment.

4.2 Visualization of Detection Chain

Before inserting the Gold foil, the performance of the readout electronics was investigated by observing the output of each module on an oscilloscope. The signal from the photodiode was observed via the output of the pre-amplifier. As shown in figure 4, the signal seen on the pre-amplifier is a falling pulse. The pre-amplifier signal is then fed to the amplifier, where it undergoes a prescribed gain and is inverted. These two pulses are shown together in figure 4. Here, the gain is set to 10, so the ampltiude of the amplifier pulse in 10 times that of the pre-amplifier pulse.

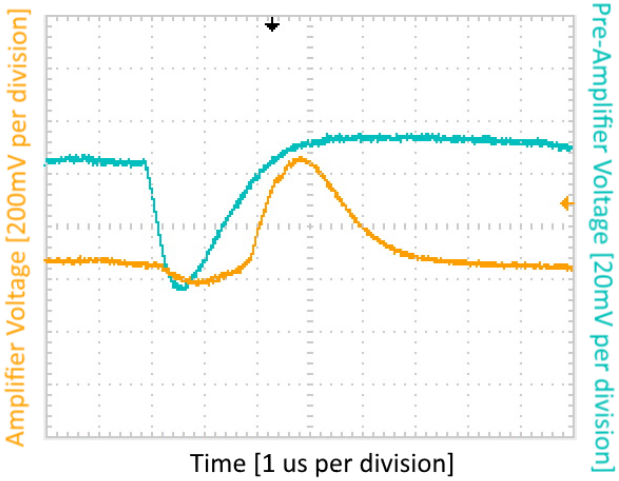

Figure 4: Signal pulse from the pre-amplifier and amplifier, as seen on the oscilloscope display

The amplifier signal is fed to the discriminator module. If the amplifier signal has an amplitude greater than the threshold prescribed by the discriminator,

then the discriminator outputs a digital pule. Figure 5 shows this digital discriminator pulse displayed over the pre-amplifier pulse. Every pulse output by the discriminator corresponds to a count on the counter module.

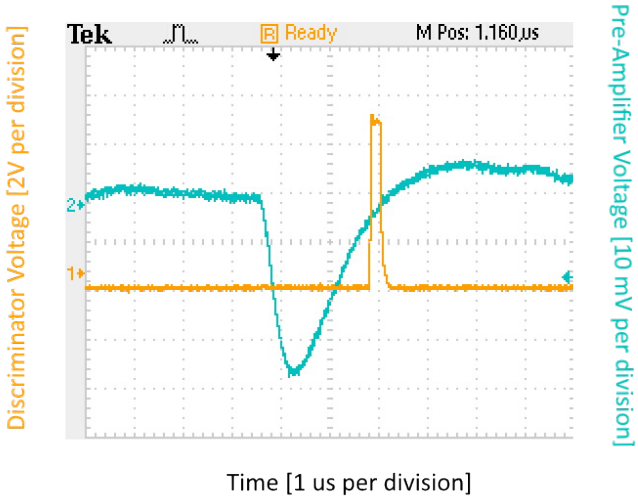

Figure 5: Signal pulse from the pre-amplifier and discriminator, as seen on the oscilloscope display

5 Data Analysis

5.1 Data Analysis I: Gold

5.1.1 Scattering Rate

While performing the experiment, the direct rate of scattered alpha particles for a particular angle over a certain period of time was determined from data straight from the counter. The direct rate, $N_d(\theta)$, was determined simply by dividing the mean number of counts by the number of seconds the counter was allowed to run. For the gold foil at an angle of $\theta = 15°$ and a time of $t = 100\,\text{s}$, the direct rate was:

$$\begin{aligned} N_d(15°) &= \frac{n_m}{t} \\ N_d(15°) &= \frac{(1.2)}{(100)} \\ N_d(15°) &= 12 \times 10^{-3} \end{aligned}$$

Similar calculations were performed for the remaining angles, and the results of those calculations, as well as the collected data, can be viewed in Figure 11.

The direct scattering rate $N_d(\theta)$, however, is only relevant to a two-dimensional plane scattering geometry, not the sought-after three-dimensional geometry.

Therefore, $N_d(\theta)$ must be extrapolated into three dimensions. In three dimensions, the alpha particles are scattered across a solid angle $d\Omega$ rather than across a two-dimensional plane. In order to take into account the third dimension, the direct scattering rate must be multiplied by the scattering angle. The result is the spacial scattering rate $N(\theta)$:

$$N(\theta) = d\Omega N_d(\theta)$$
$$N(\theta) = 2\pi \sin(\theta) N_d(\theta)$$

For the gold foil, a direct scattering rate of $N_d(15°) = 12 \times 10^{-3}$ yields a spacial scattering rate of:

$$N(15°) = 2\pi \sin(15°)(12 \times 10^{-3})$$
$$N(15°) = 19.5 \times 10^{-3}$$

Similar calculations were performed for the remaining angles, and the results of those calculations can be viewed in Figure 11. The uncertainties in the scattering rates were found by executing the Julia program displayed in Section **??**.

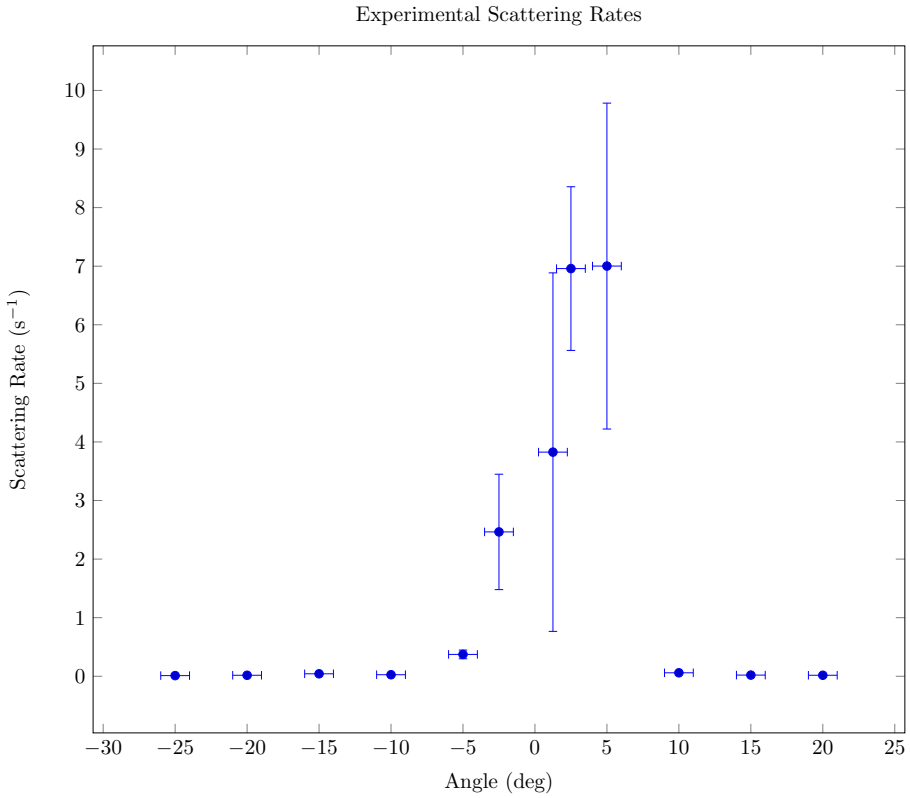

Figure 6: The plot of the experimental values for the scattering rates of the alpha particles through the foil measured at different angles.

The theoretical values for the scattering rates of the alpha particles through the gold foil were determined using Rutherford's scattering formula, $N(\theta) = N_0 n \frac{Z^2 e^4}{(8\pi\epsilon_0 E_\alpha)^2 \sin^4\left(\frac{\theta}{2}\right)}$, where N_0 is the incident particle rate, n is the nuclear density of the foil (found by multiplying the foil material's atomic concentration by the foil's thickness), Z is the nuclear number of the foil's material, E_α is the energy of the incident alpha particles, e is the elementary charge, and ϵ_0 is the dielectric constant. This formula is implemented on line 101 of the general functions source file found in Section **??**. The results of this calculation can be seen in Figure 11.

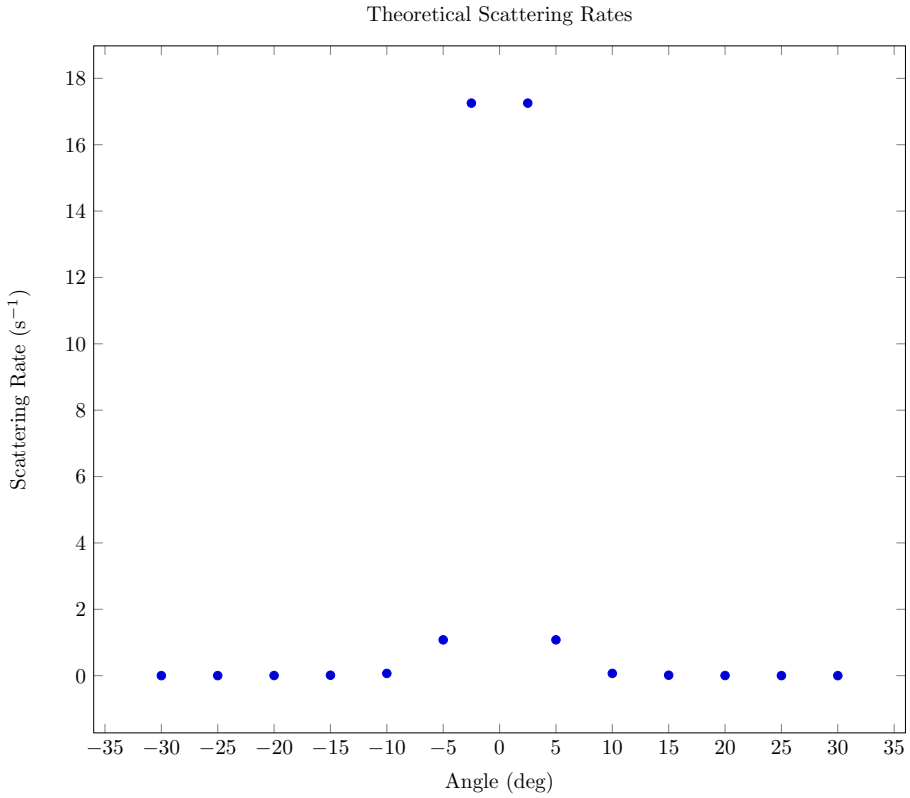

Figure 7: The plot of the theoretical values for the scattering rates of the alpha particles through the foil at different angles.

5.1.2 Differential Cross Section

The equation for finding the theoretical value of the differential cross-section is Equation 2, $\frac{d\sigma}{d\Omega}(\theta) = \left(\frac{ZZ'e^2}{4\pi\epsilon_0}\right)^2 \left(\frac{1}{4E_\alpha}\right)^2 \frac{1}{\sin^4\left(\frac{\theta}{2}\right)}$. The theoretical differential cross-section of an alpha particle emitted from an Americium-241 source incident on a gold nucleus at 15° may be calculated in the following manner:

$$\frac{d\sigma}{d\Omega}(\theta) = \left(\frac{ZZ'e^2}{4\pi\epsilon_0}\right)^2 \left(\frac{1}{4E_\alpha}\right)^2 \frac{1}{\sin^4\left(\frac{\theta}{2}\right)}$$

$$\frac{d\sigma}{d\Omega}(15^\circ) = \left(\frac{(79)(2)e^2}{4\pi\epsilon_0}\right)^2 \left(\frac{1}{4(879\,\mathrm{fJ})}\right)^2 \frac{1}{\sin^4\left(\frac{(15^\circ)}{2}\right)}$$

$$\frac{d\sigma}{d\Omega}(15^\circ) = 239.6\,\mathrm{b\,sr^{-1}}$$

Similar calculations were performed for the other incident angles using the Julia function found on line 110 in Section **??**, and the results are displayed in Figure 8.

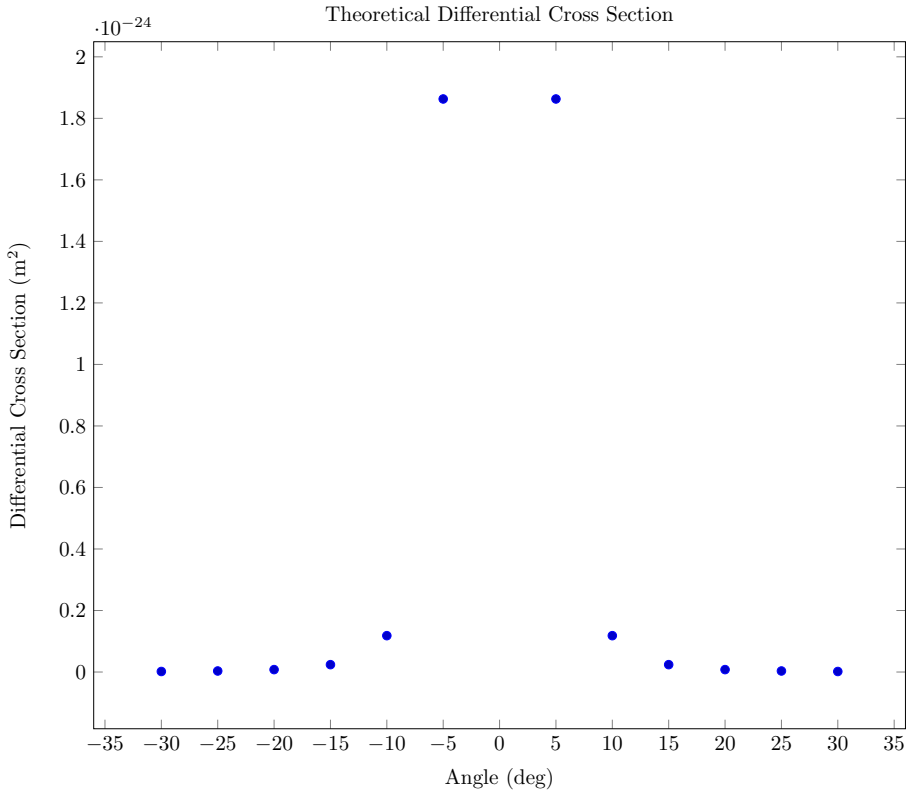

Figure 8: The theoretical values of the differential cross section of alpha particles incident on a gold nucleus at several angles.

The equation for finding the experimental value of the differential cross-section is Equation 2, $\frac{d\sigma}{d\Omega}(\theta) = \frac{\frac{dN}{dt}(\theta)}{\frac{dN_0}{dt} n \Delta\Omega}$. Information collected for $\theta = 15°$ was used to perform the calculation.

$$\frac{d\sigma}{d\Omega}(\theta) = \frac{\frac{dN}{dt}(\theta)}{\frac{dN_0}{dt} n \Delta\Omega}$$
$$\frac{d\sigma}{d\Omega}(15°) = \frac{(19.5 \times 10^{-3})}{(30.8)(1.18 \times 10^{21})(}$$

5.2 Data Analysis II: Aluminum

5.2.1 Scattering Rate

The nuclear charge number of aluminum can be determined with $Z_{\mathrm{Al}} = \sqrt{\frac{N_{\mathrm{Al}}(\theta) n_{\mathrm{Al}} Z_{\mathrm{Al}}^2}{N_{\mathrm{Au}}(\theta) n_{\mathrm{Au}}}}$, where $N_x(\theta)$ is the spacial scattering rate of alpha particles through a foil of material x at an angle θ, n_x is the nuclear density of the foil of material x (found by multiplying the foil material's atomic concentration by the foil's thickness), and Z_x is the nuclear number of material x.

The direct counting rate and the spacial counting rate were calculated in the same manner as for gold. The results of the experiment are displayed in Figure 12.

Since the nuclear charge formula requires the scattering rates of both gold and aluminum, the uncertainty for both measurements needed to be propagated through it. The uncertainty for the scattering rates through gold was calculated in the code shown in Section **??**, and the uncertainty for the scattering rates through aluminum was calculated in the code shown in Section **??**. The plots for those two calculations are shown in Figures 6 and 9 respectively. The experimental value for the nuclear number of aluminum was calculated using the code shown in Section **??**, and it was determined to be 62.7 ± 3.216.

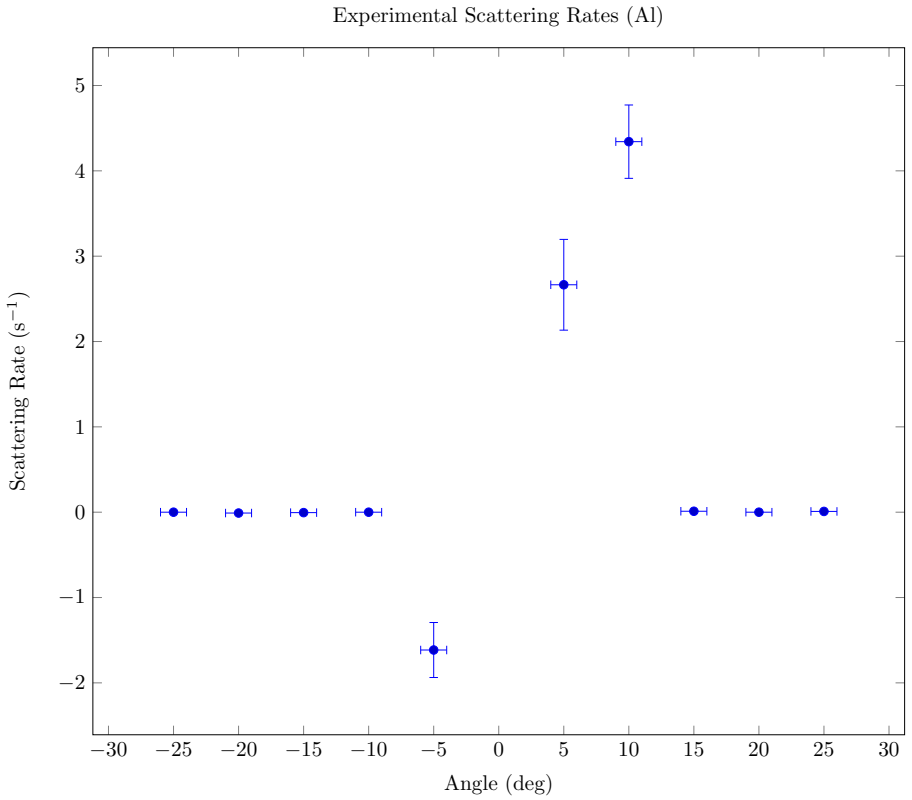

Figure 9: The plot for the experimental scattering rates of alpha particles through an aluminum foil.

The theoretical value of aluminum's nuclear charge was calculated in much the same way as the experimental, except the theoretical values of the scattering rates of the two foils were used. The theoretical values of the scattering rates through both gold and aluminum were calculated using the code shown in Sections **??** and **??** respectively, and the data is represented graphically in Figures **??** and 10. The theoretical value of the aluminum's nuclear charge was

calculated using the code shown in Section **??**, and it's value was found to be 13.

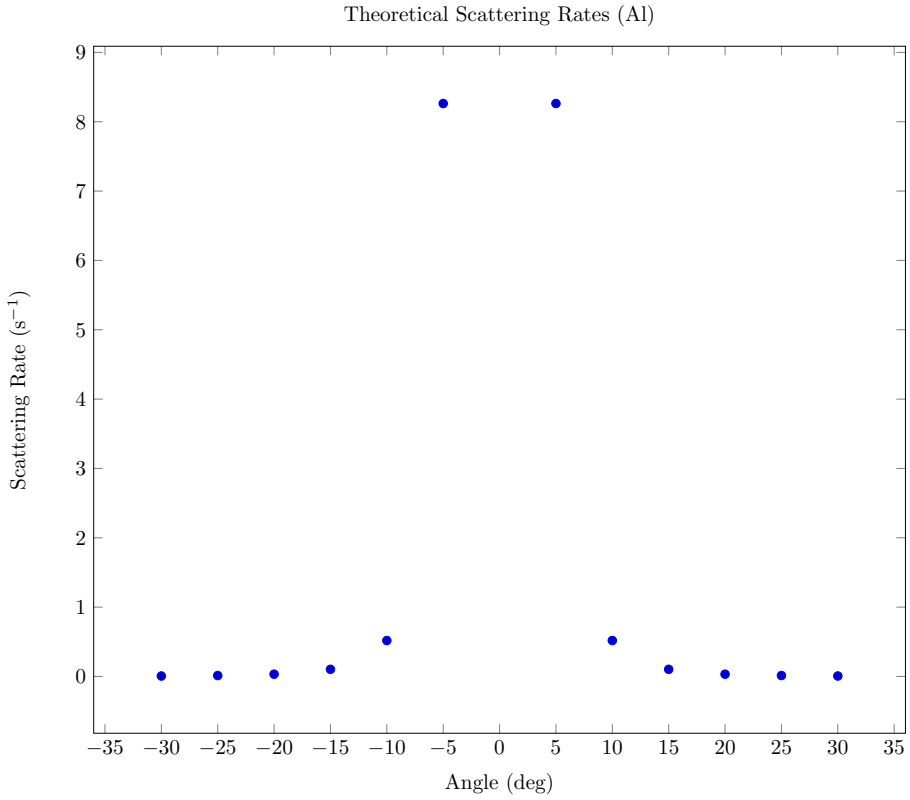

Figure 10: The plot for the theoretical scattering rates of alpha particles through an aluminum foil.

6 Results

6.1 Results I: Gold

The differential cross-section is calculated using equation 8, shown below.

$$\frac{d\sigma}{d\Omega} = \frac{\frac{dN}{dt}(\theta)}{\frac{dN_0}{dt} \times n \times \Delta\Omega} \tag{8}$$

The uncertainty in this differential cross-section measurement is propagated as follows:

$$\delta\left(\frac{d\sigma}{d\Omega}\right) = \left|\frac{d\sigma}{d\Omega}\right| \sqrt{\left(\frac{\delta dN/dt}{dN/dt}\right)^2 + \left(\frac{\delta dN_0/dt}{dN_0/dt}\right)^2 + \left(\frac{\delta n}{n}\right)^2 + \left(\frac{\delta \Delta\Omega}{\Delta\Omega}\right)^2} \tag{9}$$

Note that in equation 9, $\delta dN/dt$ and $\delta dN_0/dt$ are uncertainties in measured rates, n is a given value that can be assumed to have no uncertainty, and $\delta\Delta\Omega$ is propagated from the distance to the photodiode and the height and width of the photodiode windows as follows:

$$\begin{aligned}\Delta\Omega &= \frac{A}{r^2} \\ &= \frac{h \times w}{r^2} \\ &= \frac{(4.12 \times 10^{-3} m) \times (2.22 \times 10^{-3} m)}{(1.97 \times 10^{-2} m)^2} \\ &= 0.02 \text{ sterad}\end{aligned}$$

The uncertainties in the height, width, and distance were taken to be the standard deviation of a set of three measurements taken for each quantity.

$$\begin{aligned}\delta(\Delta\Omega) &= |\Delta\Omega| \sqrt{\left(\frac{\delta h}{h}\right)^2 + \left(\frac{\delta w}{w}\right)^2 + 2\left(\frac{\delta r}{r}\right)^2} \\ &= |0.02 \text{ sterad}| \sqrt{\left(\frac{4.75 \times 10^{-4}}{4.12 \times 10^{-3}}\right)^2 + \left(\frac{7.64 \times 10^{-5}}{2.22 \times 10^{-3}}\right)^2 + 2\left(\frac{5.01 \times 10^{-4}}{1.97 \times 10^{-2}}\right)^2} \\ &= 0.0025 \text{ sterad}\end{aligned}$$

The difference between experimental and theoretical cross-section values has an associated uncertainty. If the theoretical value is assumed to have no uncertainty, then the uncertainty associated with the difference will be that calculated in equation 9.

6.2 Results II: Aluminum

6.3 Source of Error

The Rutherford scattering chamber does not hold a perfect vacuum seal when the valve is fully closed, potentially due to a bad o-ring. The closing valve also had some issues opening and closing, so for this reason it was decided that the valve would be left open and the vacuum pump left on. Alpha particles have a much shorter lifetime in air than in a vacuum. For this reason, a poor vacuum seal that allows air to enter the chamber would result in alpha particles that decay before reaching the detector, and this would systematically lower the measured count rate. Again, this issue was combated by maintaining the vacuum inside the chamber.

Electronic noise can systematically increase the measured rate if an appropriate threshold is not set. If the threshold is too low, higher amplitude noise could be counted as "signals". The amplitude of the baseline noise was observed, and a threshold was set to remove signals below this amplitude. On the final day of data collection, the amplitude of the background noise seemed to increase from

the previous sessions, even though no characteristics of the set-up were altered. While still unclear, it was suspected that a poor cable connection was responsible for the noise. The threshold was increased to account for this increased noise level. However, the signal-to-noise ratio was still sufficiently high so that, even with the increased threshold, there was little risk of true counts falling below this threshold. However, if any lower energy alpha particles fell below this increased threshold, data taken on this data would show systematically lower rates due to the decreased counts.
The rate of scattering is dependent on the area density of the scatterers (gold nuclei), which in turn is dependent on the thickness of the foil. This parameter is assumed to be constant throughout experimentation. Any fluctuation in the thickness of the foil would therefore contribute a random intrinsic error in the density of scatterers, and by extension in the scattering rate.

7 Conclusion

8 Appendices

8.1 Appendix A: Data

8.1.1 Gold Scattering Rates

Figure 11: The found and calculated experimental and theoretical values pertaining to the scattering rate of alpha particles through gold foil.

Angle (°)	Gate Time (s)	Pulse Counts	Mean Counts	Direct Rate (s^{-1}	Spacial Rate (s^{-1})	Theoretical Rate (s^{-1})
-25	600	3 2	2.5	4.17×10^{-3}	-11.1×10^{-3}	1.78×10^{-3}
-20	200	1 0 0 2 5	1.6	8×10^{-3}	-172	4.30×10^{-3}
-15	100	1 0 0 11 1	2.6	26	-42.3×10^{-3}	13.5×10^{-3}
-10	100	3 1 3 3 2	2.4	24×10^{-3}	-26.2×10^{-3}	67.7×10^{-3}
-5	100	55 69 62 76 79	68.2	682×10^{-3}	-373×10^{-3}	1.079
-2.5	100	876 922	899	8.99	-2.46	17.25
0	100	2688 2746	2717	27.17	0	∞
2.5	100	2539	2539	25.39	6.96	17.25
5	100	1225 1352 1263 1238 1315	1278.6	12.79	7.002	1.079
10	100	5 8 4 7 3	5.4	54×10^{-3}	58.9×10^{-3}	67.7×10^{-3}
15	100	1 3 1 0 1	1.2	20 12×10^{-3}	19.5×10^{-3}	13.5×10^{-3}

Angle (°)	Gate Time (s)	Pulse Counts	Mean Counts	Direct Rate (s^{-1})	Spacial Rate (s^{-1})	Theoretical Rate (s^{-1})
		0				
		0				
		0				
		6				
20	200	2	1.6	8×10^{-3}	17.2×10^{-3}	4.30×10^{-3}
		0				
25	600	2	1	1.67×10^{-3}	4.43×10^{-3}	1.78×10^{-3}

8.1.2 Scattering Rates Aluminum

Figure 12: The collected and calculated experimental and theoretical data pertaining to the scattering rates of the alpha particles at different angles through the aluminum foil.

Angle (°)	Gate Time (s)	Pulse Counts	Mean Counts	Direct Rate (s^{-1})	Spacial Rate (s^{-1})	Theoretical Rate (s^{-1})
-25	600	0	0	0	13.6×10^{-3}	
-20	200	1	1	5×10^{-3}	-10.7×10^{-3}	32.9×10^{-3}
		0				
		1				
-15	100	0	333×10^{-3}	333×10^{-3}	-5.42×10^{-3}	103.0×10^{-3}
		0				
-10	100	0	0	0	518×10^{-3}	
		284				
		363				
		302				
		310				
-5	100	216	295	2.95	-1.615	8.263
		531				
		459				
		509				
		470				
5	100	465	486.8	4.868	2.666	8.263
		3				
		1				
10	100	3	398	3.98	4.342	518×10^{-3}
		0				
		1				
15	100	1	0.667	6.67×10^{-3}	10.8×10^{-3}	103×10^{-3}
20	200	0	0	0	0	32.9×10^{-3}
25	600	2	2	3.33×10^{-3}	8.85×10^{-3}	13.6×10^{-3}

8.2 Appendix B: Source Code